

ELECTRONIC STRUCTURE AND MAGNETIC PROPERTIES OF DOUBLE PEROVSKITES Sr_2FeMO_6 ($\text{M} = \text{Sc}, \text{Ti}, \dots, \text{Ni}, \text{Cu}$) ACCORDING TO THE DATA OF FLAPW-GGA BAND STRUCTURE CALCULATIONS

V. V. Bannikov, I. R. Shein, V. L. Kozhevnikov,
and A. L. Ivanovskii

UDC 541.16

Changes in the electronic structure and magnetic characteristics of Sr_2FeMO_6 double perovskites were studied by the FLAPW-GGA *ab initio* band structure method in relation to the type of the cation $\text{M} = \text{Sc}, \text{Ti}, \dots, \text{Ni}, \text{Cu}$.

Keywords: double perovskites Sr_2FeMO_6 , band structure, magnetism, modeling.

INTRODUCTION

Strontium ferrite SrFeO_3 has attracted considerable interest as a basic phase in developing new multifunctional materials. Among these are ceramics with conductivity of mixed ionic and electronic type, promising cathode and membrane materials, materials for oxygen sensors, so-called magnetic half-metals, materials for spin electronics (spintronics), etc. [1-9].

Doping the Fe sublattice with d metal atoms, including scandium [10], titanium [11], chromium [12], manganese [13], cobalt [14], copper [3], and a number of $4d$ and $5d$ metal atoms (see, e.g., [15-18]) is one of the basic techniques for modifying the properties of strontium ferrites. The concentration of M dopants in $\text{SrFe}_{1-x}\text{M}_x\text{O}_3$ solid solutions can reach $x \geq 0.5$ [13, 15-18], which occasionally leads to the formation of ordered Sr_2FeMO_6 phases known as *double perovskites*.

Great attention has also been paid to multication doping; some part of the sites of the strontium and iron sublattice are simultaneously replaced with different cations (e.g., $\text{La}_{0.3}\text{Sr}_{0.7}\text{Fe}_{1-x}\text{Ga}_x\text{O}_{2.65+\delta}$ type phases [19]), or the iron sublattice sites are replaced with cations of two different types (e.g., $\text{Sr}_2\text{Fe}_{1-x}\text{M}_x\text{ReO}_6$, where $\text{M} = \text{Cr}$ or Zn [20]), etc.

At the same time, the overwhelming majority of synthetic materials based on doped SrFeO_3 [1-20] have a complex variable chemical composition; moreover, many materials have structural defects and nonstoichiometry in the oxygen sublattice.

This wide set of different (and variable) factors hinders analysis of changes in the magnetic and electronic properties of the initial (SrFeO_3) matrix responsible for the physical properties of materials based on it, especially in the case of multication doping of ferrite.

The aim of the present work is to study, within a **single model**, changes in the electronic structure and magnetic properties of perovskite-like $\text{SrFe}_{1-x}\text{M}_x\text{O}_3$ phases doped with transition metals phases **depending on the type of the 3d atom** ($\text{M} = \text{Sc}, \text{Ti}, \dots, \text{Ni}, \text{Cu}$).

Institute of Solid State Chemistry, Ural Division, Russian Academy of Sciences, Yekaterinburg; ivanovskii@ihim.uran.ru. Translated from *Zhurnal Strukturnoi Khimii*, Vol. 49, No. 5, pp. 815-820, September-October, 2008. Original article submitted February 12, 2008.

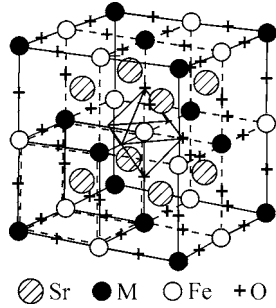


Fig. 1. Fragment of the crystal structure of Sr_2FeMO_6 double perovskite.

MODEL AND CALCULATION PROCEDURE

To study the electronic and magnetic properties of perovskite-like $\text{SrFe}_{1-x}\text{M}_x\text{O}_3$ phases depending on the type of the $3d$ dopant we used the Sr_2FeMO_6 double perovskite model (which corresponded to the formal stoichiometry of $\text{SrFe}_{0.5}\text{M}_{0.5}\text{O}_3$ solid solutions) with an fcc cell (space group $Fm\bar{3}m$), in which the component atoms occupied the following positions: M (0, 0, 0), Fe (1/2, 0, 0), Sr (1/4, 1/4, 1/4), and O (1/4, 0, 0) (Fig. 1). All metals from the $3d$ series (Sc, Ti, ..., Ni, Cu) were considered as dopant elements (M). To determine how the properties of ferrite changed with the type of the $3d$ dopant we assumed that all Sr_2FeMO_6 phases 1) retained their ordered cubic structure; 2) the oxygen vacancies were absent; and 3) the phases had ferromagnetic (FM) spin ordering.

The calculations were carried out by the full-potential augmented plane wave method (WIEN2k FLAPW code [21]) with the generalized gradient approximation (GGA) of the exchange correlation potential in the PBE form [22]. The radii of the atomic *muffin-tin* (MT) spheres were 2.00 au (Sr), 2.00 au (Fe), 1.60 au (O), 1.70 au (M = Sc–Cr), and 1.84 au (M = Mn–Cu). The set of plane waves K_{\max} was determined by the equation $R_{\text{MT}}K_{\max} = 7.0$. The integration over the Brillouin zone (BZ) was carried out by the tetrahedra method using the $10 \times 10 \times 10$ net for 47 k points in the irreducible part of the BZ of Sr_2FeMO_6 . The convergence criterion (for the total energy) was 0.0001 Ry.

RESULTS AND DISCUSSION

Band structure and magnetic moments of perovskite SrFeO_3 . The total and partial densities of state (DOS) of the cubic SrFeO_3 phase are presented in Fig. 2. In agreement with previous data (see review [23]), our calculations showed that for ferromagnetic SrFeO_3 , the spin polarization effect was most important for the $\text{Fe}3d$ bands; as a result, the energy of the d_{\uparrow} band decreased, and that of the d_{\downarrow} band increased. The magnetic moments (MMs) on iron atoms were $2.86 \mu_B$. The splitting of the $\text{Fe}3d$ states into the spatial and spin components led to their hybridization with the oxygen $2p$ states within the range from -7 eV to E_F (Fig. 2). As a result, small induced magnetic moments ($\text{MM} \sim 0.15 \mu_B$) appeared on oxygen atoms. The spin splittings of the occupied states of strontium were absent (the magnetic moment of $\text{Sr} \sim 0.01 \mu_B$). The contributions of the $\text{Sr}5s,5p$ states to the valence region of the spectrum were extremely small; i.e., strontium was in the cation form close to Sr^{2+} . As a result, the chemical bond in SrFeO_3 was a combined covalent and ionic bond; the $\text{Sr}-\text{O}$ bonds were ionic, and the $\text{Fe}-\text{O}$ bonds had both the covalent (due to hybridization of the $\text{Fe}3d-\text{O}2p$ orbitals) and ionic components (due to the partial charge transfer in the direction $\text{Fe} \rightarrow \text{O}$).

Magnetic characteristics of double perovskites Sr_2FeMO_6 (M = Sc, Ti, ..., Ni, Cu). Table 1 lists the calculated total (μ_{tot} per unit cell) and local magnetic moments (LMMs) of the component atoms in the series of Sr_2FeMO_6 double perovskites (M = Sc, Ti, ..., Ni, Cu). It can be seen that the total magnetic moment of Sr_2FeMO_6 changed (depending on the

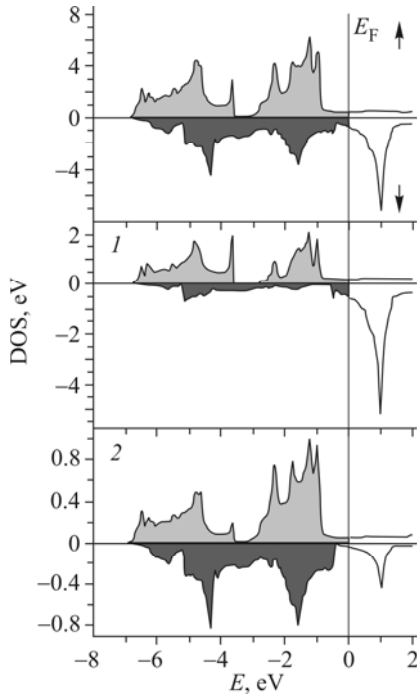


Fig. 2. Total (top) and partial spin DOS of cubic perovskite-like strontium ferrite SrFeO_3 . The spin densities are given for the $\text{Fe}3d$ (*I*) and $\text{O}2p$ (2) states (per atom).

TABLE 1. Local Magnetic Moments on Atoms (LMMs, μ_B) and Total Magnetic Moment (μ_{tot} , μ_B/cell) for Sr_2FeMO_6 Cubic Perovskite-like Phases ($M = \text{Sc}, \text{Ti}, \dots, \text{Ni}, \text{Cu}$)

Phase	LMM*				Phase	LMM*			
	M	Fe	O	μ_{tot}^{**}		M	Fe	O	μ_{tot}^{**}
$\text{Sr}_2\text{FeScO}_6$	-0.011	2.360	0.077	3.013	$\text{Sr}_2\text{FeMnO}_6$	3.108	2.656	0.107	6.998
$\text{Sr}_2\text{FeTiO}_6$	-0.040	1.661	0.050	2.017	$\text{Sr}_2\text{FeCoO}_6$	2.712	2.369	0.251	7.008
Sr_2FeVO_6	-0.157	2.929	0.068	3.251	$\text{Sr}_2\text{FeNiO}_6$	1.527	2.400	0.237	5.716
$\text{Sr}_2\text{FeCrO}_6$	1.518	3.128	0.064	5.473	$\text{Sr}_2\text{FeCuO}_6$	0.223	2.352	0.189	4.007

*The LMM of strontium is negligibly small for all phases (< 0.012 μ_B).

**The total magnetic moment recalculated per cell.

type of the $3d$ metal M) nonmonotonically and reached the maximum value $\mu_{\text{tot}} \sim 7.0 \mu_B$ for $\text{Sr}_2\text{FeMnO}_6$ and $\text{Sr}_2\text{FeCoO}_6$. For double perovskites involving metals from the early and late $3d$ series, μ_{tot} was much lower, namely, $\sim 2.0 \mu_B$ ($\text{Sr}_2\text{FeTiO}_6$), $3.0 \mu_B$ ($\text{Sr}_2\text{FeScO}_6$), and $4.0 \mu_B$ ($\text{Sr}_2\text{FeCuO}_6$).

The origin of the dependence of μ_{tot} in the series of Sr_2FeMO_6 can be understood from changes in the LMMs of the components atoms of these perovskites. As can be seen from the data of Table 1, the LMMs of strontium in all Sr_2FeMO_6 phases are negligible, while the induced LMMs of oxygen atoms change nonmonotonically and reach the maximum values for phases involving $3d$ metals from the end of the series. However, these LMMs are relatively low (up to $0.23\text{-}0.25 \mu_B$) and do not significantly affect the total changes in the magnetic properties in the series of Sr_2FeMO_6 perovskites, which primarily depend on the LMM values of the sublattices of M and iron atoms. The LMMs of iron atoms vary from $1.66 \mu_B$ ($\text{Sr}_2\text{FeTiO}_6$) to $3.12 \mu_B$ ($\text{Sr}_2\text{FeCrO}_6$), while those of $3d$ metal atoms vary from $0.01 \mu_B$ to $3.11 \mu_B$. For instance, for Sr_2FeMO_6 phases,

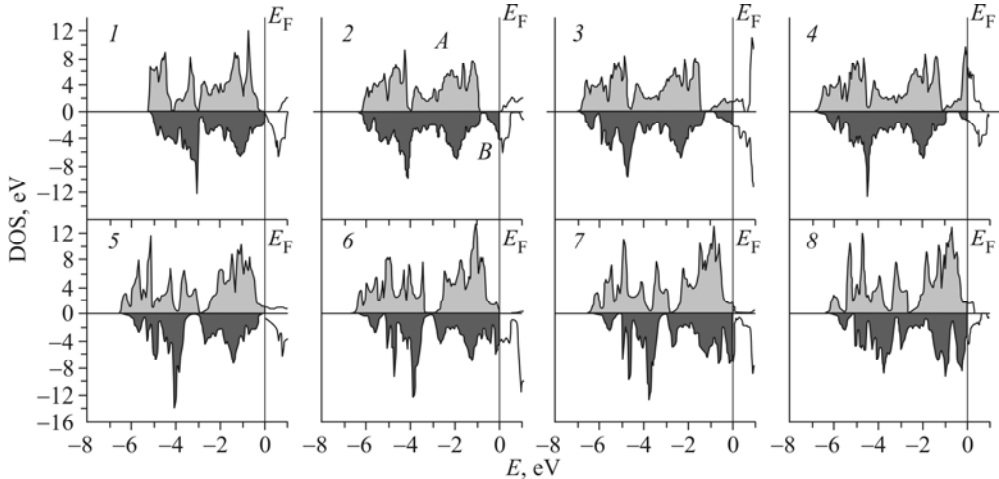


Fig. 3. Total densities of spin states for Sr_2FeMO_6 phases, where M is Sc (1), Ti (2), V (3), Cr (4), Mn (5), Co (6), Ni (7), and Cu (8).

TABLE 2. Total Densities of Spin States at the Fermi Level ($N_{\uparrow,\downarrow}(E_F)$, in states/(eV·cell)) for Sr_2FeMO_6 Cubic Perovskite-like Phases (M = Sc, Ti, ..., Ni, Cu)

Phase	$N_{\uparrow}(E_F)$	$N_{\downarrow}(E_F)$	Type of system	Phase	$N_{\uparrow}(E_F)$	$N_{\downarrow}(E_F)$	Type of system
$\text{Sr}_2\text{FeScO}_6$	0	0.044	Magnetic semiconductor	$\text{Sr}_2\text{FeMnO}_6$	1.024	0.137	Magnetic metal
$\text{Sr}_2\text{FeTiO}_6$	0	4.325	Magnetic half-metal	$\text{Sr}_2\text{FeCoO}_6$	0.047	4.536	The same
Sr_2FeVO_6	1.480	1.836	Magnetic metal	$\text{Sr}_2\text{FeNiO}_6$	1.630	7.553	»
$\text{Sr}_2\text{FeCrO}_6$	10.621	1.203	The same	$\text{Sr}_2\text{FeCuO}_6$	1.518	3.653	»

where M are 3d metals from the start of the series (Sc, Ti, and V) or Cu, the LMMs of these M atoms are small ($0.01 \mu_B$, $0.04 \mu_B$, $0.16 \mu_B$, and $0.22 \mu_B$, respectively); for the first three 3d metals, the LMMs are orientated antiparallel to the LMMs of iron atoms. Thus, the overall magnetic properties of these four perovskites depend on the magnetic properties of the iron sublattice.

For other Sr_2FeMO_6 phases, where M = Cr, Mn, Co, and Ni, the LMMs of these atoms ($1.5\text{-}3.1 \mu_B$) are close to those of iron atoms ($2.4\text{-}3.1 \mu_B$), and the M and Fe magnetic sublattices make comparable contributions to the formation of the total μ_{tot} of Sr_2FeMO_6 phases. For $\text{Sr}_2\text{FeCrO}_6$ and $\text{Sr}_2\text{FeNiO}_6$, LMM (M) is smaller than LMM (Fe), while for $\text{Sr}_2\text{FeMnO}_6$ and $\text{Sr}_2\text{FeCoO}_6$, the LMM of the M sublattices is larger than the LMM of the iron sublattice. The spin state distributions discussed below allow us to analyze the above-mentioned changes in the magnetic characteristics in the series of double perovskites Sr_2FeMO_6 .

Electronic structure of double perovskites Sr_2FeMO_6 (M = Sc, Ti, ..., Ni, Cu). The calculated spin densities of states of Sr_2FeMO_6 are given in Fig. 3; the DOS values at the Fermi level ($N(E_F)$) are presented in Table 2. It should be taken into account that the whole series of double perovskites under study can be divided (with respect to the initial SrFeO_3 phase) into two groups, namely, 1) perovskites doped with holes (Sr_2FeMO_6 , where M = Sc, Ti, ..., Mn) and 2) perovskites doped with electrons (Sr_2FeMO_6 , where M = Co, Ni, and Cu). Considering then the series of Sr_2FeMO_6 perovskites within the rigid zone model, one can state that for the first group of phases, the valence band is emptied because of the “deficiency” of electrons (relative to the valence electron concentration (VEC) per cell of the starting perovskite SrFeO_3); for the second group, where the VEC is higher than for SrFeO_3 , this band is additionally filled. Based on the form of the electronic spectrum of SrFeO_3 within this model (Fig. 1), we can expect the metal-like type of spectrum for all double perovskites.

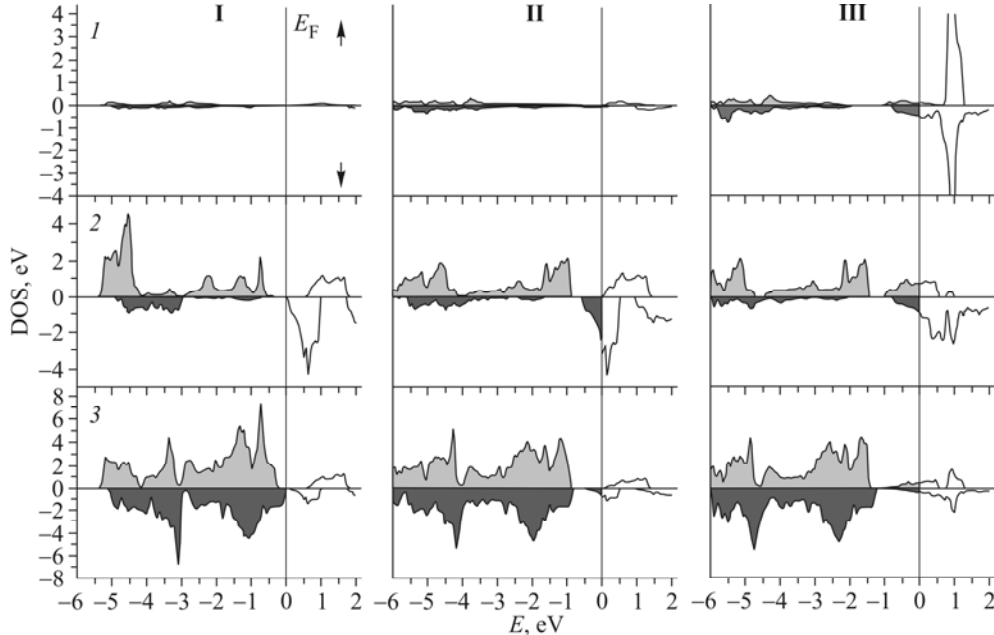


Fig. 4. Partial densities of spin states for cubic perovskite-like phases $\text{Sr}_2\text{ScFeO}_6$ (I), $\text{Sr}_2\text{TiFeO}_6$ (II), and Sr_2VFeO_6 (III). The spin densities are given for (Sc, Ti, V)3d (1), Fe3d (2), and oxygen (3).

The numerical FLAPW-GGA calculations of Sr_2FeMO_6 revealed a more complex picture (Fig. 3). In the spectrum of $\text{Sr}_2\text{FeScO}_6$, a wide forbidden gap (FG) ~ 1.0 eV is formed between the completely occupied and vacant states with the positive spin projection, while for the states with the negative spin projection, their density at the Fermi level is close to zero. Thus, $\text{Sr}_2\text{FeScO}_6$ is a gapless magnetic semiconductor. $\text{Sr}_2\text{FeTiO}_6$ has an absolutely different electronic structure. For this compound, the band of the states with the positive spin projection (band *A*, Fig. 3) is completely occupied and has an FG, while for the band with the negative spin projection, its upper vacant (for $\text{Sr}_2\text{FeScO}_6$) edge (subband *B*, Fig. 3) starts to be filled at increased VECs. As a result, the spectrum of $\text{Sr}_2\text{FeTiO}_6$ is of the metallic type for one spin subsystem (carrier density at the Fermi level is $N_{\downarrow}(E_F) > 0$), but contains a forbidden gap for the opposite spin projection ($N_{\uparrow}(E_F) = 0$). These materials with 100% spin polarization of the near-Fermi electrons are known as magnetic half-metals (review [9]). All other Sr_2FeMO_6 perovskites have nonzero density of carriers at the Fermi level for both spin subsystems ($N_{\uparrow,\downarrow}(E_F) > 0$, Table 2) and are magnetic metals.

The formation of the above-mentioned three types of magnet (magnetic semiconductor, half-metal, and metal) can be traced in detail in Fig. 4, which gives the partial DOS of double perovskites involving 3d metals from the start of the series, $\text{Sr}_2\text{FeScO}_6$, $\text{Sr}_2\text{FeTiO}_6$, and Sr_2FeVO_6 . It can be seen that for $\text{Sr}_2\text{FeScO}_6$, the contribution of the Sc 3d states to the region of the occupied band is small, and the valence band is mainly formed from the Fe3d $_{\uparrow,\downarrow}$ and O2p states. Remarkably, the upper edge of the valence band of this phase is composed of only O2p $_{\downarrow}$, and the lower edge of the conduction band, of mixed Fe3d $_{\downarrow}$ -O2p $_{\downarrow}$ states.

On passing to $\text{Sr}_2\text{FeTiO}_6$, the admixture of the Ti3d states in the valence band remains insignificant, while an increase in VEC leads to the occupation of the lower part of the Fe3d $_{\downarrow}$ -O2p $_{\downarrow}$ band. The spectrum of the electronic states of this phase becomes half-metallic, $N_{\downarrow}(E_F) > 0$ and $N_{\uparrow}(E_F) = 0$.

After Sr_2FeVO_6 , further evolution of the spectrum of double perovskites is determined by two factors, namely, growth of VEC (progressive occupation of the valence band) and considerable contributions of the M3d $_{\uparrow,\downarrow}$ states to the valence band. Figures 3 and 4 show that for Sr_2FeVO_6 , the peak of the density of the V3d $_{\uparrow,\downarrow}$ states is ~ 1 eV higher than E_F , while for $\text{Sr}_2\text{FeCrO}_6$, the peak of the density of states of chromium lies directly in the region of E_F , making the maximum

contribution to $N_{\uparrow}(E_F)$ (Table 2). As the number of the $3d$ element increases, the orbital energy decreases; i.e., the density of the $M3d_{\uparrow,\downarrow}$ states is shifted deep into the valence band. As VEC increases, the band of the $M3d_{\uparrow}$ states and then the band of the $M3d_{\downarrow}$ states are occupied (Fig. 3), which determines the tendency of variation of the LMM in the series of Sr_2FeCrO_6 phases.

CONCLUSIONS

Using the FLAPW-GGA *ab initio* band structure method we analyzed changes in the electronic and magnetic properties of cubic perovskite-like phases Sr_2FeMO_6 , where $M = Sc, Ti, \dots, Ni, Cu$.

It was found that **depending on the type of the $3d$ atom,**

- 1) the Sr_2FeMO_6 phase can be one of the three types of magnet (magnetic semiconductor, half-metal, or metal);
- 2) the magnetic properties of Sr_2FeMO_6 phases, where $M = 3d$ metals from the start of the series (Sc, Ti, and V) or Cu, are determined by the magnetic properties of the iron sublattice;

3) the magnetic properties of Sr_2FeMO_6 phases, where $M = Cr, Mn, Co$, and Ni, are determined by comparable contributions from the magnetic sublattices of M and iron atoms; the local magnetic moments of M atoms are either larger (Sr_2FeMnO_6 and Sr_2FeCoO_6) or smaller (Sr_2FeCrO_6 and Sr_2FeNiO_6) than the magnetic moments of iron atoms;

4) the tendencies in the formation of the electronic spectrum and the magnetic characteristics of Sr_2FeMO_6 phases depend on two factors: valence electron concentration (per perovskite cell) and the number (orbital energy of the $3d$ states) of the M atom. The first factor regulates the total occupancy of the valence band of Sr_2FeMO_6 ; the second determines the admixture of $M3d_{\uparrow,\downarrow}$ states in the valence band of strontium ferrite.

At the next stage, we will study the dependence of changes in the properties of doped ferrites on the concentration of $3d$ dopants and the presence of oxygen vacancies, which can substantially affect the functional characteristics of real synthesized materials.

This work was supported by the “Hydrogen energetics” program of the Russian Academy of Sciences.

REFERENCES

1. M. V. Patrakeev, I. A. Leonidov, V. L. Kozhevnikov, and V. Kharton, *Solid State Sciences*, **6**, No. 9, 907-913 (2004).
2. N. N. Oleynikov and V. A. Ketsko, *Russ. J. Inorg. Chem.*, **49**, Suppl. 1, S1-S21 (2004).
3. X. Zhang, X. F. Dong, and W. M. Lin, *J. Inorg. Mater.*, **22**, No. 1, 97-100 (2007).
4. A. Rothschild, S. J. Litzelman, H. L. Tuller, et al., *Sensors Actuators*, **108**, Nos. 1/2, 223-230 (2005).
5. E. Carvajal, O. Navarro, R. Allub, et al., *Eur. Phys. J.*, **B48**, No. 2, 179-187 (2005).
6. I. R. Shein, V. L. Kozhevnikov, and A. L. Ivanovskii, *Pisma Zh. Éksp. Teor. Fiz.*, **82**, No. 4, 239-242 (2005).
7. I. R. Shein, V. L. Kozhevnikov, and A. L. Ivanovskii, *Fiz. Tekh. Poluprovodn.*, **40**, No. 11, 1295-1299 (2006).
8. B. Fisher, J. Genossar, K. B. Chashka, et al., *Curr. Appl. Phys.*, **7**, No. 2, 151-155 (2007).
9. A. L. Ivanovskii, *Usp. Fiz. Nauk*, **177**, No. 10, 1083-1105 (2007).
10. A. A. Markov, M. V. Patrakeev, V. V. Kharton, et al., *Chem. Mater.*, **19**, No. 16, 3980-3987 (2007).
11. E. V. Tsipis, M. V. Patrakeev, V. Kharton, et al., *Solid State Sci.*, **7**, No. 4, 355-365 (2005).
12. Q. Ming, J. Hung, Y. L. Yang, et al., *Combustion Sci. Technol.*, **138**, Nos. 1-6, 279-296 (1998).
13. H. J. Lee, G. Kim, J. S. Kang, et al., *J. Appl. Phys.*, **101**, No. 9, art. 09G523 (2007).
14. A. Munoz, J. A. Alonso, M. J. Martinez-Lope, et al., *J. Solid State Chem.*, **179**, No. 11, 3365-3370 (2006).
15. W. Zhong, W. Liu, X. L. Wu, et al., *Solid State Comm.*, **132**, Nos. 3/4, 157-162 (2004).
16. J. Herrero-Martin, J. Garcia, G. Subias, et al., *J. Phys.: Cond. Matter.*, **16**, No. 39, 6877-6890 (2004).
17. F. Sher, A. Venimadhav, M. G. Blamire, et al., *Chem. Mater.*, **17**, No. 1, 176-180 (2005).
18. T. S. Chan, R. S. Liu, G. Y. Guo, et al., *Solid State Comm.*, **133**, No. 4, 265-270 (2005).

19. M. V. Patrakeev, E. B. Mitberg, A. A. Lakhtin, et al., *J. Solid State Chem.*, **167**, No. 1, 203-213 (2002).
20. A. Jung, I. Bonn, V. Ksenofontov, et al., *J. Mater. Chem.*, **15**, No. 17, 1760-1768 (2005).
21. P. Blaha, K. Schwarz, G. K. H. Madsen, et al., in: *WIEN2K, An Augmented Plane Wave Plus Local Orbitals Program for Calculating Crystal Properties*, K. Schwarz (ed.), Techn. Universität Wien, Austria (2001).
22. J. P. Perdew, S. Burke, and M. Ernzerhof, *Phys. Rev. Lett.*, **77**, No. 18, 3865-3868 (1996).
23. I. R. Shein, K. I. Shein, V. L. Kozhevnikov, and A. L. Ivanovskii, *Fiz. Tverd. Tela*, **47**, No. 11, 1998-2003 (2005).